

# Computer Microtomography of Zircon: A New Approach to the Selection of Targets for U–Pb Geochronologic Studies

Yu. V. Plotkina, E. B. Sal'nikova, A. B. Kotov, M. D. Tolkachev, and M. R. Pavlov

*Institute of Precambrian Geology and Geochronology, Russian Academy of Sciences, nab. Makarova 2, St. Petersburg, 199034 Russia*

*e-mail: Julia@IK4843.spb.edu*

Received June 14, 2005

**Abstract**—The paper reports results obtained by the complex studying of zircon crystals from rocks of various genesis. Zircon is one of the minerals most often used as geochronometers. It also provides genetic information on superimposed processes that is “recorded” in the external and internal morphology of its crystals. This mineral is thoroughly examined to select its unaltered crystals for U–Pb dating by the single-grain method. Zircon grains are selected with the use of optical and electron microscopy and cathodoluminescence. This publication presents the first results obtained by examining zircon by computer microtomography ( $\mu$ CT) and the results of the studying of the external and internal structure by conventional techniques ([optical microscopy and SEM (SE and CL)]. The paper demonstrates the advantages of the application of the  $\mu$ CT techniques to the selection of targets for U–Pb zircon dating: there is no need for the special preparation of the samples and no material is destructed. However, this technique may be not informative enough if the zircon contains inherited core whose density does not differ from the density of the surrounding mineral.

**DOI:** 10.1134/S0869591106020044

Modern techniques of U–Pb geochronology make it possible to date not only grains of accessory minerals but also their fragments (Poller *et al.*, 1997, 2002; and others), which sets strong requirements for the techniques used for the preparatory examination of the crystals. In the course of a geochronologic research, minerals used as geochronometers, first of all, zircon, are commonly examined by electron microscopy, Raman spectroscopy (RMP; Nasdala *et al.*, 1998), and cathodoluminescence (CL), which is traditionally considered to be the most informative (Varva, 1994; Poller *et al.*, 2002; Kempe *et al.*, 2004). However, these methods have certain limitations and require the preparation of the samples, a procedure that is usually associated with the loss of significant part of the material to be studied. Moreover, the interpretation of the results of these studies may sometimes be ambiguous, as is the case with zircon affected by polycyclic transformations or with that mineral with inherited more ancient radiogenic Pb.

The heterogeneity of natural single crystals is largely caused by the imperfectness of their crystal structure (or some of its fragments), which is related in zircon to radiation-induced disturbances. Inner fragments of a crystal with different crystallinity can be identified by BSE and CL only fairly roughly, and only when the original structure is almost completely destroyed.

A method that makes it possible to reveal minute differences between the densities of objects on a submi-

rometer-sized scale is computer microtomography ( $\mu$ CT). This publication presents the results of microtomographic studies of crystals of zircon, a mineral used as a geochronometer. The microtomographic results are compared with the data obtained by other techniques.

Zircon crystals were examined optically under a Laborlux 12 POLs microscope (Germany). The morphology of the crystals was studied on an ABT-55 scanning electron microscope (Japan) equipped with a Link 10 000 (Great Britain) analytical system. The crystals were sputter coated with gold (a layer  $\sim 100$  Å thick). The zircon crystals were also studied by CL on a Cam-Scan 2300 MV scanning electron microscope equipped with a Centaurus detector (accelerating voltage 15 kV). The microtomographic research was conducted on a SkyScan-1072 microtomograph at the universities of Ghent and Antwerp (Belgium). The construction of the microtomograph and the study method are described in detail in (Sasov and Van Dyck, 1998). The microtomographic study involves the stepwise obtaining of sets of 2D images that are then processed with the ANT program ([www.skyscan.be](http://www.skyscan.be)) to construct a 3D model for the density structure of the object with a spatial resolution of 2  $\mu$ m. The precision of this method in application to our objects is 10–15%.

The technique of microtomography was tested on zircon crystals of various age and with variable inner structures, which were either highly crystalline or partly metamict. The brief characteristics of the samples, their geological settings, and the estimated U–Pb

**Table 1.** Morphological features of zircon crystals

Sample	Morphological characteristics	Geologic setting and age (U–Pb zircon dating)
KRN-007	Euhedral prismatic crystals, transparent, pale pink, with abundant mineral inclusions	Granite, Kyrinskii Massif, Transbaikalia, $173 \pm 2$ Ma (unpublished data of the authors)
Sh-7	Subhedral short-prismatic (up to rounded) crystals, transparent, lilac	Subalkaline granite, Sharyzhalgai block of the Siberian platform basement, $1870 \pm 4$ Ma (Sal'nikova <i>et al.</i> , 2003)
SShB-1270	Euhedral prismatic crystals, turbid, "rusty" in color, face surfaces are corroded, contain metamictized cores	Granite, Bain-Khuduk (Avdaratinskii) Massif, Mongolia, $290 \pm 8$ Ma (unpublished data of the authors)
V-1	Subhedral short-prismatic (up to rounded) translucent crystals, contain inclusions	Alkaline granite, Vishnevogorsk, Urals
A-134	Euhedral prismatic crystals, transparent, yellowish, contain inclusions	Granite, Dzhugdzhur–Stanovik folded area, $136 \pm 1$ Ma (Larin <i>et al.</i> , 2003)
5813	Subhedral prismatic crystals, semitransparent, dark cherry in color, with single inclusions	Vein pegmatoid granite, Sharyzhalgai block of the Siberian platform basement, $2557 \pm 28$ Ma (Sal'nikova <i>et al.</i> , 2003)
201	Euhedral prismatic crystals, semitransparent, pink, with gas and mineral (ore) inclusions	Metadacite, Balaganakh greenstone belt, Aldan Shield, $2017 \pm 25$ Ma (unpublished data of the authors)

ages of the zircon crystals are presented in Table 1, and the results of the comparative study of their inner structures by various methods ( $\mu$ CT, SEM, CL, and optical microscopy in transmitted light) are summarized in Table 2.

Samples KRN-007, SShB-1270, and Sh-7 (Table 2) are the most illustrative for the comparison of the results obtained with various methods for the inner structures of the crystals. In application to them, the  $\mu$ CT technique allowed us to reveal inner structural features that could not be identified by transmitted-light microscopy or cathodoluminescence. For example,  $\mu$ CT managed to determine that crystal no. 1 from sample KRN-007 includes a zone of unevenly distributed elevated density, which was not identified by the optical and CL methods. Crystal no. 5 was determined to bear numerous large ( $\sim 20$   $\mu$ m) apatite inclusions (the mineral was identified by microprobe analyses), which were not visible in either transmitted light or cathodoluminescence.

In the transparent zircon from sample Sh-7 (Table 7), which was homogeneous in transmitted light, CL has revealed a core with partly disturbed fine zoning and an unzoned thin crystalline outer shell with lower luminescence. The results of  $\mu$ CT scanning point to the existence of at least three zones of different densities (Table 2). The outermost zone (I) corresponds to the outer shell identified by cathodoluminescence, and the inner zones (II and III) correspond to domains with different densities (and, perhaps, also with various crystallinity).

Our  $\mu$ CT examination of zircon from sample SShB-1270 has definitely revealed two zones of different density, which generally correspond to transparent and semitransparent crystal portions visible in transmitted light and two zones of elevated luminescence and disturbed zoning detected by cathodoluminescence. It is

pertinent to mention that only the results of  $\mu$ CT allowed us to propose an unambiguous interpretation for the complicated CL image of the inner structures of these crystals. For example, the outer zone with bright CL in crystal no. 2 could be misinterpreted as a newly formed outer shell. The 3D model of the inner structure of this crystal indicates that this is most probably a large grain fragment characterized by disturbed crystallinity.

Crystals nos. 1 and 2 from sample V-1 are transparent and homogeneous in transmitted light. However, the results of CL and  $\mu$ CT indicate that the inner morphology of these crystals is perturbed, and the crystals have inherited cores (no. 2) of heterogeneous density and contain, in the central parts, domains with changed densities (nos. 1 and 2).

It should be mentioned that the method of computer microtomography may be not informative enough if the crystals have inherited cores or their relics whose density is only insignificantly different from the density of the surrounding crystal. Such an example is provided by zircon from sample A-134, in which  $\mu$ CT reveals fragments of heterogeneous density that correspond only to swarms of inclusions but not the boundaries of the core that was identified by CL (Table 2).

Thus, the comparative analysis of the results obtained on the inner structures of the crystals has demonstrated that optical examination, cathodoluminescence, and microtomography can be applied as mutually complementary techniques, whose use can enable the researcher to eliminate uncertainties in the interpretation of the inner morphology of zircon crystals. Inasmuch as  $\mu$ CT is a method that does not destroy the sample, it is expedient to utilize this technique among the first when crystals are selected for geochronologic studies. This makes it possible to preserve the original material (which is crucial when U–Pb dating is con-

**Table 2.** External and internal morphology of zircon crystals


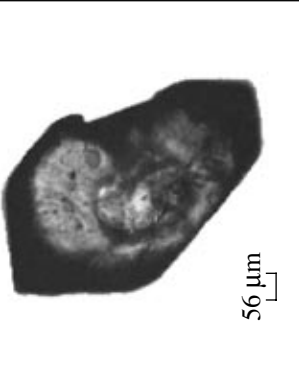
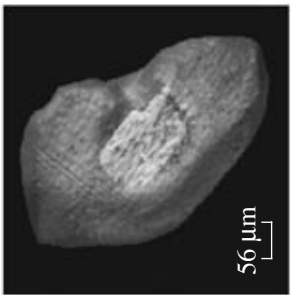
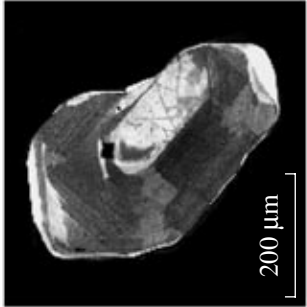

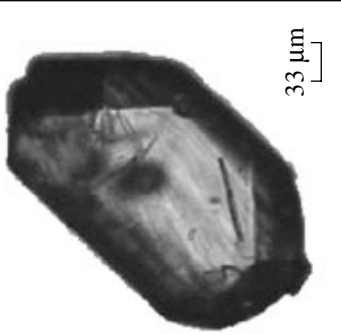

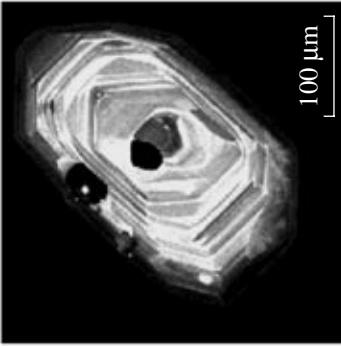
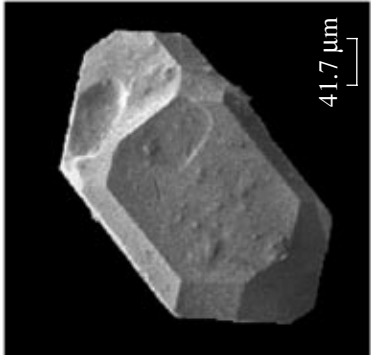
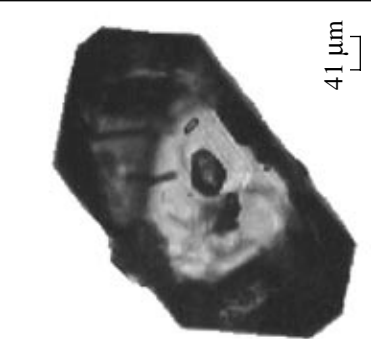
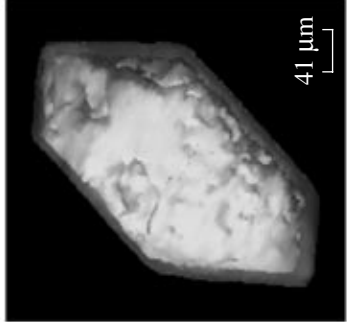
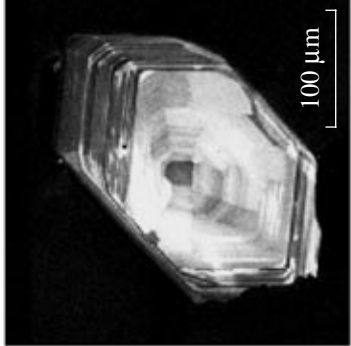
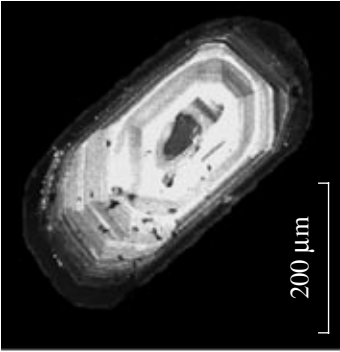
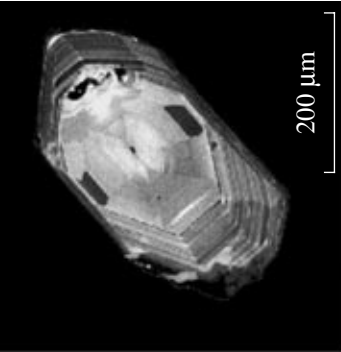
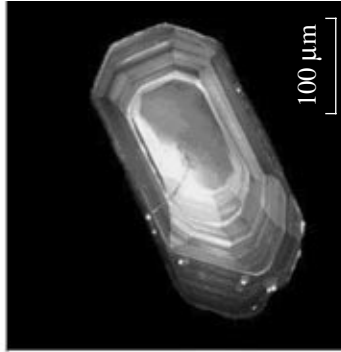

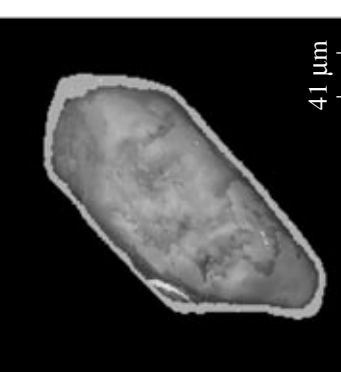
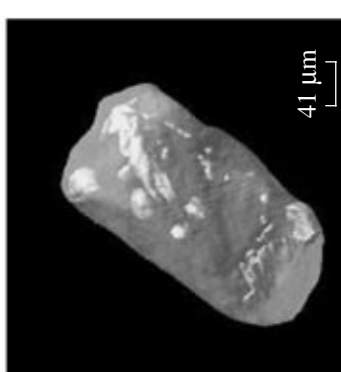

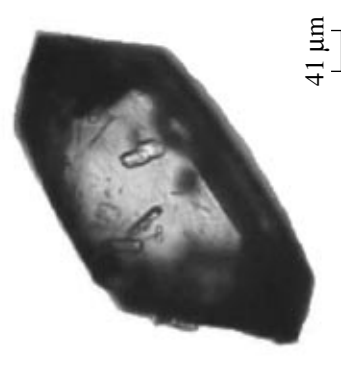
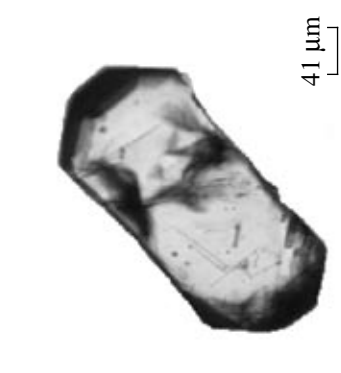
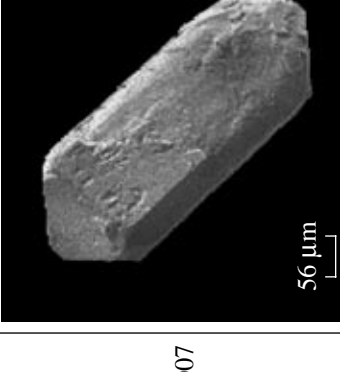


Sample (crystal)	SEM (SE)	Optical microscopy (transmitted light)	$\mu$ CT	SEM (CL)
5813				
KRN-007 (1)				
KRN-007 (2)				

Table 2. (Contid.)

		
		
		
		
<p>KRN-007 (3)</p>	<p>KRN-007 (4)</p>	<p>KRN-007 (5)</p>

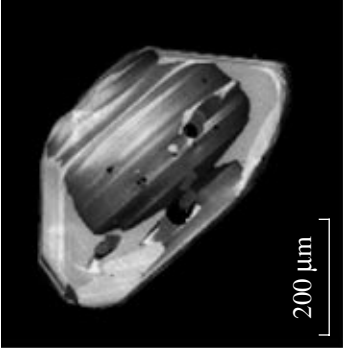
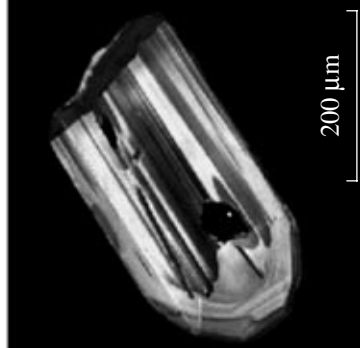

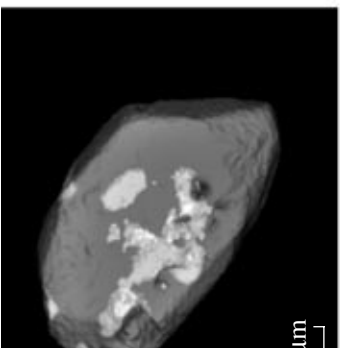


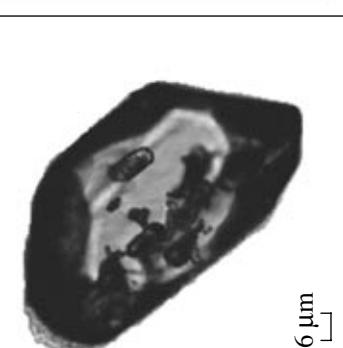
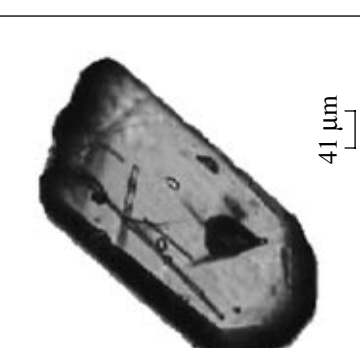

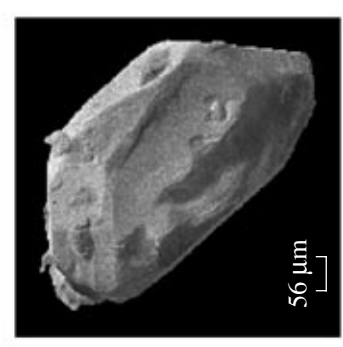

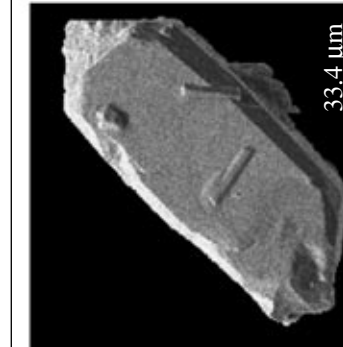
 <p>200 <math>\mu\text{m}</math></p>	 <p>200 <math>\mu\text{m}</math></p>	 <p>100 <math>\mu\text{m}</math></p>
 <p>56 <math>\mu\text{m}</math></p>	 <p>41 <math>\mu\text{m}</math></p>	 <p>33 <math>\mu\text{m}</math></p>
 <p>56 <math>\mu\text{m}</math></p>	 <p>41 <math>\mu\text{m}</math></p>	 <p>33 <math>\mu\text{m}</math></p>
 <p>56 <math>\mu\text{m}</math></p>	 <p>41.7 <math>\mu\text{m}</math></p>	 <p>33.4 <math>\mu\text{m}</math></p>
<p>A-134 (1)</p>	<p>A-134 (2)</p>	<p>SShB-1270 (1)</p>

Table 2. (Contd.)

**Table 2.** (Contd.)

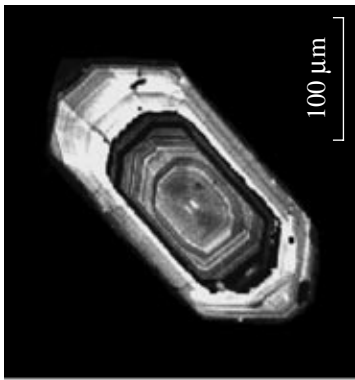
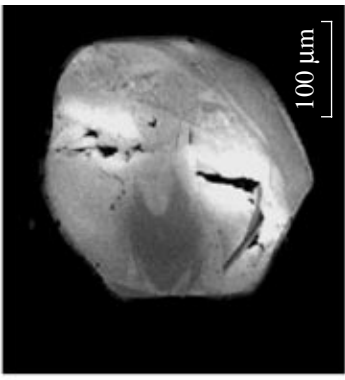
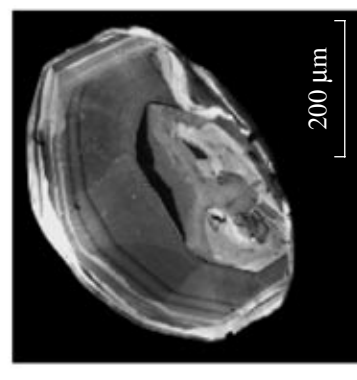
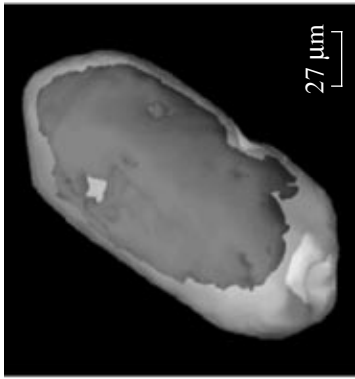
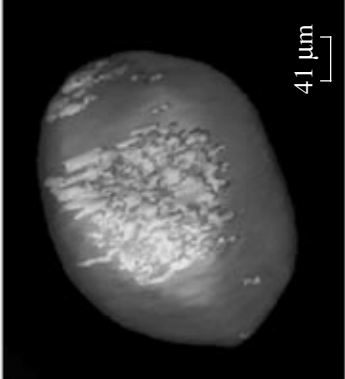
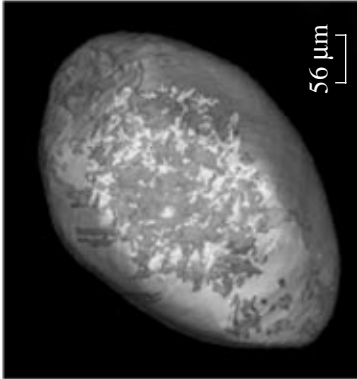



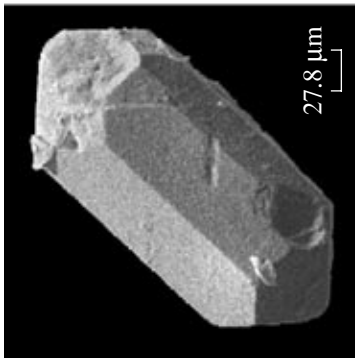
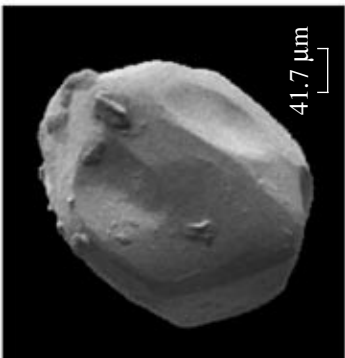
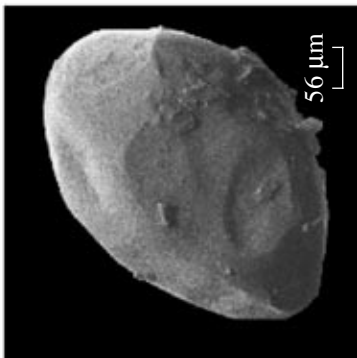
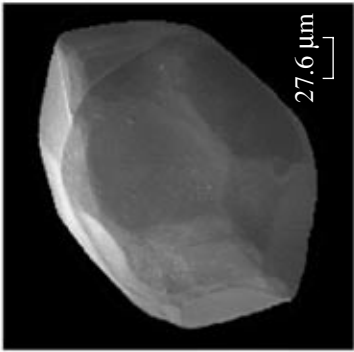
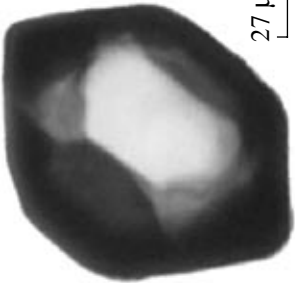
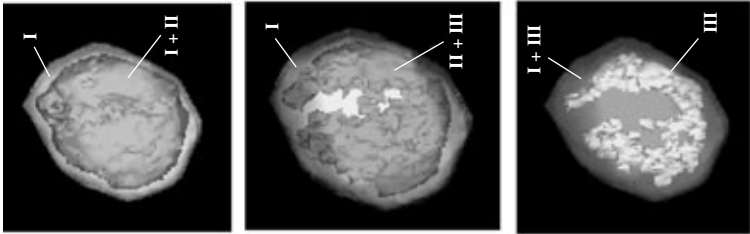
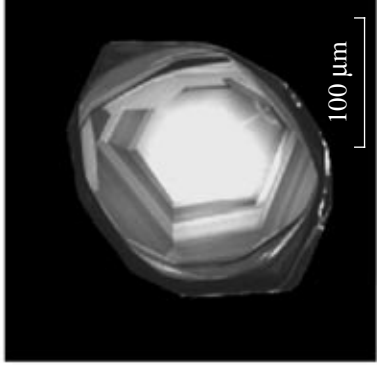



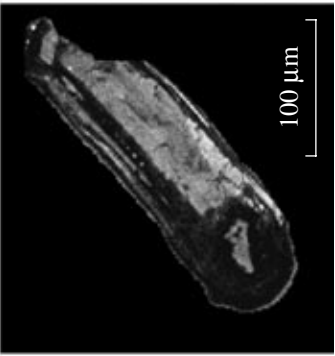
		
		
		
		
SShB-1270 (2)	V-1 (1)	V-1 (2)

Table 2. (Contd.)

<p>Sh-7</p>				
<p>201</p>				

Note: The microphotographs presented in this table reflect the inner and external morphology of zircon grains. The images were obtained by the following methods: (1) electron microcopy (crystal faceting and surface topography of crystal faces); (2) transmitted-light optic microscopy (occurrence of inclusions and their distribution); (3) microtomography (distribution of domains differing in density in the crystals, the occurrence of inherited cores); (4) cathodoluminescence (zoning, sectorial zoning, and the occurrence of inherited cores).

ducted on single grains) and avoid the special preparation of the samples. An analytical spot is selected to measure the isotopic composition of zircon on a SHRIMP ion-ion microprobe with the use of CL images of the crystal. As was demonstrated above, it is quite probable that the spot selected for this purpose is located at a mineral inclusion or within a zone with disturbed structure, which have not been identified by CL.

#### ACKNOWLEDGMENTS

The authors thank A.Yu. Sasov (Skyscan, Belgium) for help and support provided during the morphological research. This study was financially supported by the International Association for the Promotion of Cooperation with Scientists from the New Independent States of the Former Soviet Union (YSF-2001/02-085) and the Russian Foundation for Basic Research (project nos. 03-05-64893 and 04-05-64810), the Program for the Support of Leading Research Schools (NSH-615.2003.05), and the Program of Fundamental Research of the Division of Earth Sciences, Russian Academy of Sciences (programs "Geodynamic Evolution of the Lithosphere in the Central Asian Foldbelt: From a Paleocean to a Continent" and "Isotopic Geology: Geochronology and Material Sources"), and the Foundation for Assistance to National Science.

#### REFERENCES

1. U. Kempe, K. Bombach, D. Matukov, *et al.*, "Pb-Pb and U-Pb Zircon Dating of Subvolcanic Rhyolite as a Time Marker for Hercynian Granite Magmatism and Sn Mineralization in the Eibenstock Granite, Erzgebirge, Germany: Considering Effects of Zircon Alteration," *Miner. Deposita* **39**, 646–669 (2004).
2. A. M. Larin, A. B. Kotov, E. B. Sal'nikova, *et al.*, "Tectonic Evolution of the Central Part of the Dzhug-Dzhur-Stanovoi Fold System: Evidence from U-Pb Geochronological and Isotope-Geochemical (Nd, Sr, Pb) Studies," in *Isotope Geochronology in Solving Problems of Geodynamics and Ore Genesis* (TsIK, St. Petersburg, 2003), pp. 253–257 [in Russian].
3. L. Nasdala, R. T. Pigeon, and D. Wolf, "Heterogeneous Metamictization of Zircon on a Microscale," *Geochim. Cosmochim. Acta* **60** (6), 1091–1097 (1996).
4. U. Poller, V. Liebetrau, and W. Todt, "U-Pb Single-Zircon Dating under Cathodoluminescence Control (CLC-Method): Application to Polymetamorphic Orthogneisses," *Chem. Geol.* **139** (1–4), 287–297 (1997).
5. U. Poller, Th. Geisler, J. Huth, *et al.*, "Understanding CL in Natural Zircons," in *Proceedings of Goldschmidt Conference, Davos, Switzerland, 2002* (Davos, 2002), p. A 609.
6. E. B. Sal'nikova, A. B. Kotov, V. I. Levitskii, *et al.*, "Age Boundaries of High-Temperature Metamorphism in Crystalline Complexes of the Sharyzhalgai Block of the Siberian Platform," in *Isotope Geochronology in Solving Problems of Geodynamics and Ore Genesis* (TsIK, St. Petersburg, 2003), pp. 453–455 [in Russian].
7. A. Sasov and D. van Dyck, "Desktop X-Ray Microscopy and Microtomography," *J. Microscopy* **191** (2), 151–158 (1998).
8. G. Vavra, "Systematics of Internal Zircon Morphology in Major Variscan Granitoid Types," *Contrib. Mineral. Petrol.* **117** (4), 331–344 (1994).